J Solid State Electrochem (2007) 11: 65–70
DOI 10.1007/s10008-005-0070-2

ORIGINAL PAPER

Arvydas Survila · Dalia Bražinskienė

Inhibition activity of ethyleneglycol and its oligomers on tin electrode

Received: 30 June 2005 / Revised: 20 July 2005 / Accepted: 13 September 2005 / Published online: 29 November 2005

Abstract Voltammetry and electrochemical impedance spectroscopy were applied to investigate the inhibition activity of ethyleneglycol and its oligomers on tin electrode in strong acidic sulfate solutions. Tetraethyleneglycol was found to be the most active substance among compounds $HO–(CH_2–CH_2–O)_m–H$ ($m \leq 4$) that retards diffusion-controlled Sn(II) reduction due to its inhibitive adsorption. This rather slow process is controlled both by diffusion and electrosorption steps. A comparison of exchange current densities obtained in the presence of different polyethers shows that the length of the hydrocarbon chain is the main factor responsible for inhibition activity of such substances on tin electrode.

Keywords Ethyleneglycol oligomers · Tin · Adsorption · Voltammetry · Impedance

Introduction

Plating baths used for deposition of tin or its alloys usually contain surface-active substances (SASs), a wide variety of which may be seen, e.g., from the list of compounds given in [1]. First of all, different polyethers should be mentioned as the SAS suitable for improvement of tin plating. Polyethylene and polypropylene glycols (PEG and PPG, respectively) are among the most widely used polyethers. Another example might be laprol 2402 C (the bloc copolymer of PEG and PPG), which has been applied as an effective SAS for bright bronze plating [2, 3]. The substance $C_nH_{2n+1}–O–(C_2H_4–O–)_mH$, which is known as sintanol DS-10 in Russia or Pegepal C in Germany, should be also mentioned among the SAS under discussion. Distinct from the above polyethers, this substance contains a comparatively long hydrocarbon radical and acts as an effective wetting agent and inhibitor for the plating of tin and its alloys [3, 4].

Inhibition activity of such substances was found to be conditioned by various factors, depending, first of all, on the nature of substrate. For instance, laprol exhibited no pronounced effect on the kinetics of Cu(II) reduction in halide-free solutions [5], whereas the completely opposite effect of strong inhibition was observed in the case of Sn (II) reduction [6]. Similar regularities have been also observed in the case of PEG adsorption. Although some contradictory data concerning PEG surface activity on copper substrates have been reported in earlier publications (see the reviews provided by Stoychev and Tsvetanov [7, 8]), it is now possible to conclude that PEG inhibition activity on copper substrate is rather low when Cu(II) solutions are carefully protected from traces of chlorides [9]. In contrast, strong inhibitive adsorption of PEG has been detected in the case of tin reduction, and a significant decrease in the process rate attaining two to three orders of magnitude has been observed [10].

Another interesting phenomenon consists of the fact that the inhibition activity of the SAS under discussion is very sensitive to the presence of small (micromolar) amounts of halides [9]. At the same time, a quite different effect of halides, viz. halide-enhanced adsorption of laprol on copper [5, 9] and halide-suppressed its surface activity on tin [6, 9], has been observed.

The mechanism of electrode processes involving such SAS has not yet been sufficiently explored. According to impedance data [11], Sn(II) reduction in the presence of sintanol includes some steps, the nature of which is dependent on the electrode potential. An adsorption of sintanol on tin substrate has been described quantitatively by Frumkin isotherm using the values of surface coverage obtained from both voltammetric and impedance data [12].

Investigations involving PEG of different molecular masses have shown that the halide-enhanced inhibitive adsorption on copper depends not only on PEG concentration [7] but also on the length of hydrocarbon chain [13]. Recently, we managed to establish that too-short molecules cannot be classified as SAS overall. Specifically, no per-

A. Survila (✉) · D. Bražinskienė
Institute of Chemistry,
A. Goštauto 9,
01108 Vilnius, Lithuania
e-mail: arvydass@ktl.mii.lt

ceptible inhibition has been observed in Cu(II) solutions involving mono-, di-, or triethyleneglycols even in the presence of halides [14]. It has been found that only tetraethyleneglycol (TEG) HO–(CH_2–CH_2–O)$_4$–H or other derivatives with a higher molecular mass can give rise for inhibition of Cu(II) reduction.

We failed to find in the available literature any similar information concerning tin substrates. Undoubtedly, such data could be valuable for further understanding of Sn(II) reduction in general, and, particularly, of Sn and Cu co-deposition in the presence of polyethers. Experimental data obtained by using voltammetry (VA) and electrochemical impedance spectroscopy (EIS) are presented and discussed in this article.

Experimental

The solutions under investigation contained 0.01 M $SnSO_4$ (Fluka, Germany) with chloride impurities less than 0.01%, 1 M H_2SO_4 (high purity) and different amounts of ethyleneglycol and its oligomers (used as received) with general formula HO–(CH_2–CH_2–O)$_m$H, where m varied from 1 to 4. Thrice-distilled water was used for the preparation of solutions, which were deaerated with an argon stream over 0.5 h.

Voltammetric measurements were carried out using the conventional rotating disc technique with a potential scan rate of 5 mV s^{-1}. A Pt disc with 1 cm^2 surface area was used as a substrate to prepare working electrodes. It was coated at 10 mA cm^{-2} with 2- to 4-μm-thick copper sublayer in the solution containing (g dm^{-3}) $CuSO_4$ 5 H_2O, 200; and H_2SO_4, 50. Afterwards, 5- to 7-μm smooth tin coating was deposited at 10 mA cm^{-2} in the solution containing (g dm^{-3}) $SnSO_4$, 50; H_2SO_4, 160; and sintanol, 1. Similar procedures were applied to prepare the electrodes for impedance measurements. A Pt wire with a 0.36-cm^2 surface area was used in this case. Working electrodes were rinsed with water, immediately immersed into the solution under investigation, and kept in the solution for controlled time τ before measurements. A saturated Ag|AgCl, KCl electrode served as reference. To protect the solutions from Cl^- traces, a chloride-free electrolytic junction was used and changed after each experiment. Electrode potentials (E) were converted to the standard hydrogen scale. All experiments were performed at 20°C.

Impedance measurements were carried out under potentiostatic conditions at the open-circuit potentials within the frequency (f) range from 0.1 to 5×10^4 Hz using a Zahner Elektrik (Germany) IM6 impedance spectrum analyzer. Computer programs elaborated by Boukamp [15] were used for analyzing impedance spectra.

Results and discussion

As has been noticed above, TEG is the shortest molecule among PEGs that displays an inhibitive adsorption on copper substrate in the presence of halides. According to [14, 16], the existence of three ethereal oxygen atoms in a TEG molecule creates favorable conditions for the formation of pseudocrown complexes with adsorbed Cu^+ ions. However, it is still unclear whether similar chemical interactions can occur between TEG and Sn^{2+} ions, although some potentiometric data are indicative of such possibility.

The open-circuit potential of Sn electrode (E_{oc}) in SAS-free 0.01 M Sn(II) solutions containing 1 M H_2SO_4 is equal to −0.242±0.001 V and obeys the Nernst equation [12]. Corrosion of tin is able to shift the equilibrium potential to more positive values, and this shift (ΔE) depends mainly on the ratio (r) of exchange current densities of Sn|Sn^{2+} and H_2|H^+ couples ($i_{0,Sn}$ and $i_{0,H}$ respectively). According to [17], $i_{0,H}\approx10^{-11}$ A cm^{-2} for Sn electrode in 1 N H_2SO_4 solution saturated with hydrogen, i.e., this quantity is ten orders of magnitude lower than $i_{0,Sn}$ (see below). Analysis of simple voltammetric corrosion diagram shows that $\Delta E<1$ μV at $r=10^{10}$. Moreover, this shift does not exceed 1 mV even at $r>1{,}500$. This gives grounds to treat the above E_{oc} as equilibrium potential. Mono- or diethyleneglycol does not actually affect this quantity, whereas small but quite reproducible ΔE are observed on the addition of TEG, viz. −4 and −8 mV at 0.01 and 0.02 M of TEG, respectively. Such negative shifts might arise from the formation of monoligand Sn(II) complex with stability constant K_1 approximately 57 M. However, this preliminary conclusion needs more exhaustive testing, invoking other methods.

Inhibition activity of the ethyleneglycols can be judged from impedance data shown in Fig. 1. As we have established earlier [6, 9], Nyquist plots (dependencies of the imaginary part of the impedance Z'' on real part Z') obtained for SAS-free solutions at open-circuit potentials are nothing else than lines that were observed over almost the entire range of applied frequencies. This means that Sn(II) reduction is mainly controlled by diffusive mass transport. According to the different literature data [6, 9, 12, 18, 19], an exchange current density, i_0, is in the range from 50 to

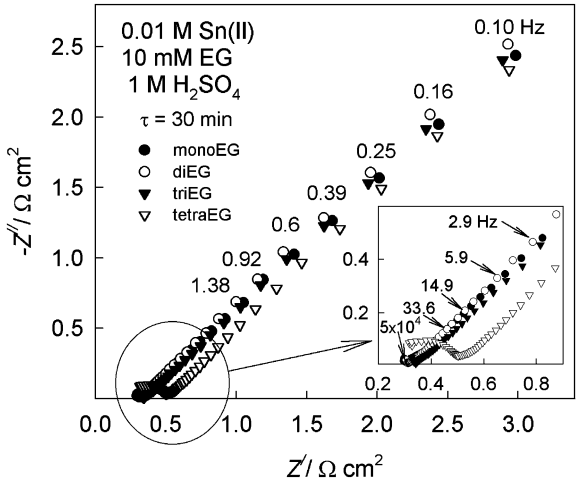

Fig. 1 Nyquist plots obtained for solutions of indicated composition at exposure time τ=30 min. The *encircled region* is expanded in the *inset*. Applied frequencies in hertz are given at some experimental *points*

250 mA cm^{-2}. The shape of Nyquist plots does not actually change on the addition of mono-, di-, or triethyleneglycols. Close straight lines with unit slope are also observed in this case. According to the analysis of the impedance spectra (the details are given bellow), quite close values of the exchange current density (84±4 mA cm^{-2}) were detected for these solutions. Only TEG shows an increased surface activity, giving rise to a small semicircle at high frequencies of alternative current (inset in Fig. 1) with i_0=46 mA cm^{-2}. Such plots are typical of the processes, the rate of which is controlled by charge transfer and diffusive mass transport simultaneously.

An inhibitive adsorption of different polyethers is usually manifested in the decreasing of cathodic current density i [6, 9, 12, 20]. A similar effect is also typical of TEG-containing solutions (Fig. 2). In the absence of this SAS, the height of a well-defined plateau of limiting current i_{lim} is in linear dependence on the square root of angular rotating velocity Ω (inset in Fig. 2) and obeys the Levich equation with diffusion coefficient D=6.1×10^{-6} cm^2 s^{-1}. An addition of TEG retards Sn(II) reduction over the entire range of cathodic overvoltages. This is also reflected in the decrease of the limiting current density, although the "$i_{lim} - \sqrt{\Omega}$" plots are still close to the lines passing through the origin (inset in Fig. 2). It should be noted that in the case of more active SAS such as laprol [6, 9, 20] or sintanol [12], the effect of the intensity of forced convection weakens with the SAS concentration (c_{SAS}), and i_{lim} ceases at all to depend on Ω at sufficiently high c_{SAS}. At the same time, the shape of voltammograms changes; specific maxima arise at low cathodic polarizations.

Considering that TEG shows the highest inhibition activity among other oligomers under investigation, the main attention was focused further on the adsorption behavior of this substance. To gain a better understanding of this point, Sn(II)-free solutions were investigated primarily. The results obtained show that the adsorption of TEG was a rather slow process: it can last an hour and does not attain an equilibrium state. Dynamics of Sn electrode impedance may be seen from Figs. 3 and 4. One measurement (starting at 50 kHz and finishing at 0.1 Hz) usually takes approximately 4.5 min, but the most part of this time (~3 min) falls on the last seven points related to the lowest (less than 1 Hz) frequencies. This means that some drift in surface properties may occur during one record of the impedance spectrum. At the same time, some instability of the subject under investigation might be considered as moderate and incapable of making serious problems in the analysis of experimental data. This gives grounds to apply proper equivalent circuits, treating the values of their elements as slightly averaged quantities.

At short exposure times (τ<20 min) and relatively low TEG concentrations (c_{TEG}=5 mM), the major part of Nyquist plots consists of straight lines with slopes equal to 1.05–1.09, i.e., close to 1 (Fig. 3). Some rudiment of semicircle can be distinguished at τ=15 min in the region of the highest frequencies (3<f<50 kHz). This part of Nyquist plots becomes more pronounced and expands with τ. Nevertheless, the semicircle remains relatively small even at long exposure times (inset in Fig. 3). Similar effects are also observed at higher (20 mM) TEG concentration (Fig. 4), with the difference that the radii of semicircles are about tenfold longer.

The shape of the plots under discussion is well known. Similar characteristics are typical of the so-called Ershler–Randles equivalent circuit consisting of two parallel subcircuits. The first of them should contain the resistance R and Warburg impedance W in series, and the latter is the single capacitance C. According to Boukamp [15], the description code of such circuit should be written as ([RW]C). Here, elements in series are given in square brackets, and

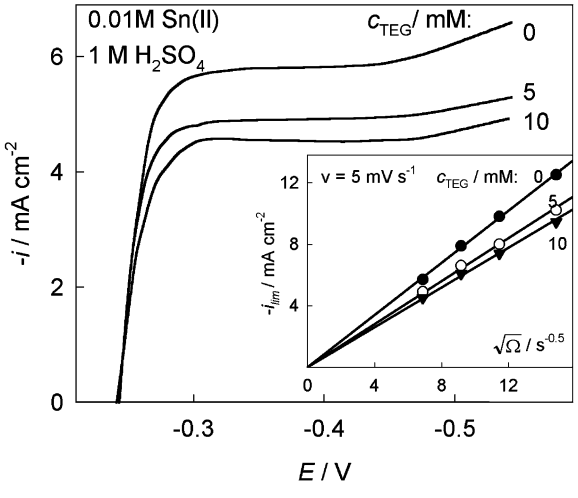

Fig. 2 Voltammograms of Sn(II) reduction recorded at 450 rpm in 0.01 M Sn(II) and 1 M H_2SO_4 solutions with different amounts of TEG indicated at the *curves*. Dependencies of limiting current density on $\sqrt{\Omega}$ (Ω is the angular velocity of rotating disc electrode) are shown in the *inset*

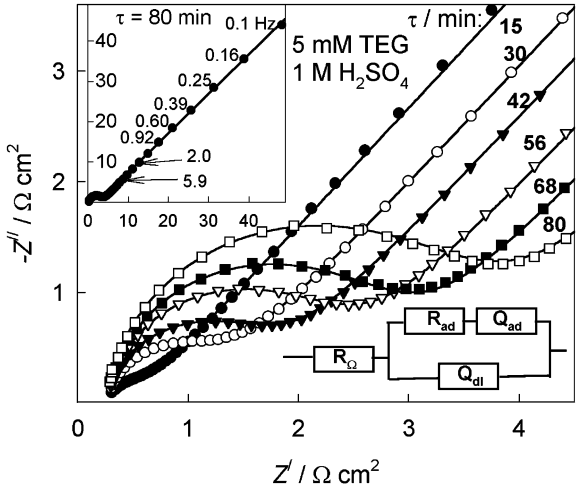

Fig. 3 Nyquist plots obtained for Sn(II)-free solution of indicated composition at open-circuit potential E_{oc}=−0,286±0.001 V and different exposure times τ designated at the respective *curves*. A high-frequency region is shown in the main *graph*, and an example of the whole plot is given in the *inset*. The *values* of applied frequencies are given at some experimental *points*. Experimental data (*symbols*) and plots simulated for shown equivalent circuit $R_\Omega([R_{ad}Q_{ad}]Q_{dl})$ (*lines*) are compared

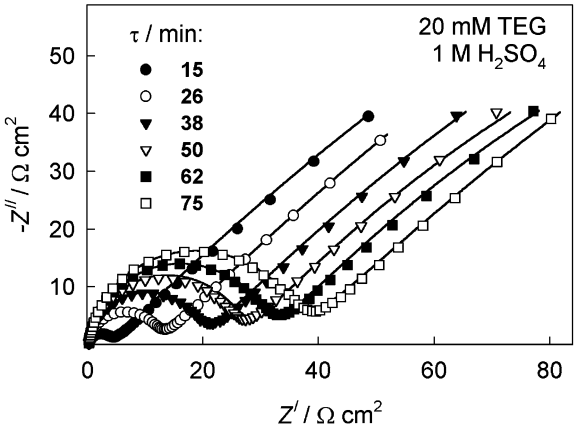

Fig. 4 Nyquist plots obtained for Sn(II)-free solution of indicated composition at open-circuit potential E_{oc}=−0,286±0.001 V and different exposure times τ. Experimental data (*symbols*) and simulated plots (*lines*) are compared

elements in parallel are enclosed in parentheses. Further, such a basic circuit may be improved and modified by adding some extra elements. Various versions of the circuits suitable for the quantitative description of adsorption phenomena have been considered, e.g., in [21, 22].

The analysis has shown that the impedance spectra obtained for Sn(II)-free solutions can be described with frequency error less than 1.5% by means of somewhat modified equivalent circuit $R_\Omega([R_{ad}Q_{ad}]Q_{dl})$ (Figs. 3 and 4). The ohmic resistance of the solutions R_Ω was found to be actually independent of c_{TEG} and equal to 0.25±0.01 Ω cm^2. The adsorption resistance R_{ad} and the constant phase element (CPE) Q_{ad} are introduced to characterize the adsorption kinetics, and the CPE Q_{dl} stands for nonideal double layer capacitance. The complex conductivity of CPE is equal to $Y_0(j\omega)^n$, where $j=\sqrt{-1}$ and $\omega=2\pi f$. The exponent n may acquire different values that characterize the nature of CPE [23].

The values of exponent n obtained for Q_{dl} lie between 0.92 and 0.96, i.e., they are close to 1. Thus, it may be said that CPE represents the double layer capacitance that is distributed along the interface due to inhomogeneity of the electrode surface. As distinct from this case, the values of n=0.5±0.02 were obtained for Q_{ad}. Therefore, this CPE should be treated as the Warburg-like impedance arising from a slow diffusion that accompanies the overall process of TEG adsorption. It is necessary to emphasize that Y_0 shows no regular dependence on c_{TEG} or τ in this case and is equal to 0.021±0.002 Ω^{-1} cm^{-2} s$^{0.5}$. According to the adsorption model proposed by Frumkin and Melik-Gaikazyan [24] and its further developments [25–30], the Warburg-like impedance may be described in terms of diffusion relaxation time $\tau_D=(\partial\Gamma/\partial c)_E^2/D$. At sufficiently low surface coverage, most isotherms show a linear relationship between adsorption Γ and SAS concentration. This can result in constant $\partial\Gamma/\partial c$ and, consequently, in constant Y_0.

The presence of adsorption resistance R_{ad} shows that the formation of adsorption layer proceeds with a finite rate v. This step of adsorption is usually modeled with a $[R_{ad}C_{ad}]$ subcircuit [21, 24, 27–30], where the resistance R_{ad} depends on $(\partial\Gamma/\partial v)_{E,c}$ and varies inversely with the adsorption rate constant [24, 25, 27–29]. We did not succeed to obtain sufficiently reliable values of C_{ad}. It is only possible to state that this capacitance is presumably rather high, approximating some millifaraday per square centimeter. Due to this, no kinetic parameters of the electrosorption process were available for us.

To obtain the values of the effective double-layer capacitance C_{dl}, we made use of the Eq. 5 given in [31] that, in our notation, takes the form: $C_{dl}=\left(Y_0R_\Omega^{1-n}\right)^{1/n}$. The results of this estimation are given (Fig. 5). Two cases of C_{ad} and R_{ad} dynamics may be distinguished. At low concentrations of TEG, slow variations of R_{ad} with time are accompanied by the fast decrease in the double-layer capacitance. Such behavior might be attributed to the initial stages of the adsorption process that are characterized by a relatively low surface coverage and a rather high adsorption rate. Different variations are observed at higher concentrations of TEG. Even at τ=20 min, C_{dl} is three to four times lower than in the former case, and further, it varies only weakly with exposure time. It may be concluded that the main formation of adsorption layer takes less than 20 min. A further increase in the adsorption resistance shows that the adsorption rate considerably falls when an equilibrium state is approached.

The addition of Sn(II) into the solutions under investigation does not actually affect the shape of Nyquist plots but decreases tenfold the total impedance (cf. Figs. 3, 4, and 6). Now, to account for the Sn(II) reduction process, the proper subcircuit should be added in parallel to the adsorption impedance. At the same time, this necessary operation poses some problems in the analysis of experimental data. The point is that the adsorption parameters established in Sn(II)-free solutions cannot be used as such in the presence of Sn(II). Therefore, a new separate analysis of a full equivalent circuit should be performed in the latter case. Usually, an increased number of circuit elements

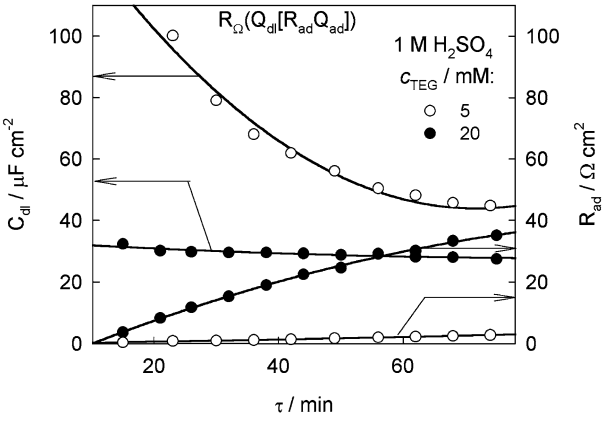

Fig. 5 Variations of double-layer capacitance C_{dl} (*ordinate to the left*) and adsorption resistance R_{ad} (*ordinate to the right*). Sn electrode was kept for a time τ in 1 M H_2SO_4 solutions containing 5 (*empty circles*) and 20 mM (*full circles*) of TEG

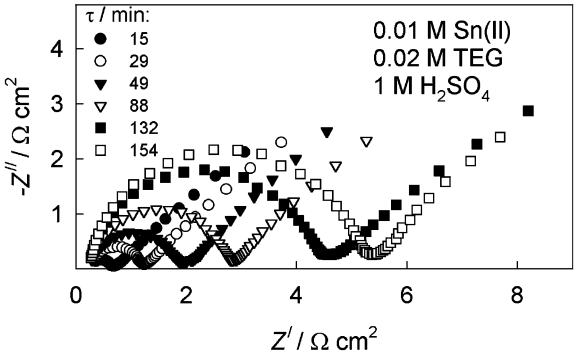

Fig. 6 Nyquist plots obtained for Sn(II) solution of indicated composition at different exposure times τ

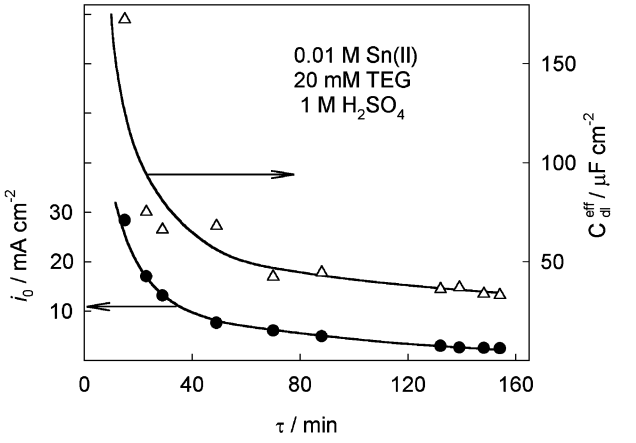

Fig. 7 Variations of the exchange current density i_0 (*ordinate to the left*) and the effective double-layer capacitance C_{dl}^{eff} (*ordinate to the right*). Sn electrode was kept for a time τ in Sn(II) solution of indicated composition

implies increased errors and reduces the reliability of the analysis. To bypass this difficulty, an approach presented in [12] was utilized. It consists of some simplification of the adsorption impedance, replacing it by single CPE, viz. Q_{dl}. Such a procedure works well when the adsorption impedance is much higher than that of the faradaic process [12].

Based on the above reasoning, the $R_\Omega([R_{ct}Q_d]Q_{dl})$ equivalent circuit was applied with the charge transfer resistance R_{ct} and the diffusion impedance Q_d. A theoretical analysis of such a circuit containing CPE has been performed by Retter et al. [32]. This circuit fits the experimental data, with frequency error less than 2%. The ohmic resistance R_Ω=0.24±0.01 Ω cm^2 remains the same as in the absence of Sn(II). Time-independent parameters of Q_d were found to be as follows: Y_0=0.37±0.02 Ω^{-1} cm^{-2} s^n, with n=0.48±0.02. The value of Warburg coefficient calculated for 0.01 M Sn(II) solution with D=6.1×10^{-6} cm^2 s^{-1} is equal to 0.384 Ω^{-1} cm^{-2} s$^{0.5}$; it fairly coincides with the quantities of Y_0 established above. The exponent n obtained for Q_{dl} varies between 0.88 and 0.91, this being indicative of the capacitive character of the double-layer impedance.

In contrast to R_Ω and Q_d, other elements (R_{ct} and Q_{dl}) vary with time. These effects are shown in Fig. 7, where the values of the exchange current density, obtained from the well-known equation $R_{ct}=RT/2Fi_0$, are given. The values of the effective double-layer capacitance C_{dl}^{eff} were obtained using the parameter Y_0 and procedures [31] accounting for the existence of both R_Ω and R_{ct}. The data in Fig. 7 show an obvious correlation between the structure of double layer and kinetics of Sn(II) reduction. The decrease in double-layer capacitance with time seems to arise from the progressive saturation of the interface with adsorbed TEG, causing the increasing inhibition of tin reduction. This manifests itself in the respective lowering of the exchange current density. More than a tenfold fall of i_0 is observed after 2 h, as compared with the SAS-free solution.

In closing, a comparison of inhibition activity of some different polyethers can be made on the basis of the exchange current densities obtained in the presence of laprol [6], sintanol [12], and TEG in the present article. Since i_0 depends on both SAS concentration and the length of hydrocarbon chain, the values of i_0 should be respectively normalized. Considering similar structure of the SAS under discussion, the number of ethereal oxygen atoms was chosen for this purpose. One elementary chain in laprol or sintanol molecule contains approximately 24 and 9–11 such atoms, respectively, whereas this quantity is only 3 in the case of TEG. A standardization of i_0 in respect to 1 mol of ethereal oxygen shows that the inhibition activity of laprol and sintanol is approximately of the same order, but this characteristic is approximately 2,000 times lower in the case of TEG. This result shows that the length of hydrocarbon chain is a prime factor responsible for inhibition activity of polyether on tin electrode.

Conclusions

Voltammetric and EIS data show that TEG is the most active surfactant among oligomers with general formula: HO–(CH$_2$–CH$_2$–O)$_m$–H (m≤4). An inhibitive adsorption of TEG retards diffusion-controlled Sn(II) reduction in strong acidic sulfate solutions and results in the respective decrease in double-layer capacitance (C_{dl}). Impedance spectra obtained for Sn(II)-free solutions are indicative of a rather slow formation of the adsorption layer. This process was found to be controlled both by diffusion and electrosorption steps. An obvious correlation between exchange current densities (i_0) and C_{dl} was detected for Sn(II)-containing solutions; both these quantities decrease with exposure time due to the progressive formation of the adsorption layer. A comparison of i_0 values obtained in the presence of different polyethers shows that the length of the hydrocarbon chain is the main factor responsible for inhibition activity of such substances on tin electrode.

Acknowledgement We are grateful to Dr. M. Samulevičienė for her kind assistance in performing impedance measurements.

References

1. Meibuhr S, Yeager E, Kozawa A, Hovorka F (1963) The electrochemistry of Sn. Effects of nonionic addition agents on electrodeposition from stannous sulfate solutions. J Electrochem Soc 110:190
2. Galdikienė O, Mockus Z (1994) Cathodic process in copper–tin deposition from sulphate solutions. J Appl Electrochem 24:1009
3. Mockus Z (1995) Electrochemical codeposition of copper and tin in acid sulphate solutions. Ph.D. Thesis Vilnius
4. Medvedev GI, Tkachenko NA (1984) Electrodeposition of copper–tin alloy from sulphate electrolyte in the presence of sintanol DS-10. Zashchita Metallov 3:484
5. Survila A, Mockus Z, Kanapeckaitė S, Samulevičienė M (2002) Adsorption behaviour of laprol 2402 C on copper electrode. Polish J Chem 76:983
6. Survila A, Mockus Z, Kanapeckaitė S (2002) Adsorption behaviour of laprol 2402 C on a tin electrode. Trans IMF 80:85
7. Stoychev D, Tsvetanov CJ (1996) Behaviour of poly(ethylene glycol) during electrodeposition of bright copper coatings in sulfuric acid electrolytes. J Appl Electrochem 26:741
8. Stoychev D, Tsvetanov CJ (1998) On the role of poly(ethylene glycol) in deposition of galvanic copper coatings. Trans IMF 26:73
9. Survila A, Mockus Z, Kanapeckaitė S (2003) Effect of halides on adsorption properties of polyether laprol 2402 C on copper and tin electrodes. J Electroanal Chem 552:97
10. Glarum SH, Marshall JH (1983) Admittance study of the Sn electrode. J Electrochem Soc 130:1088
11. Medvedev GI, Trubnikova ON (1984) Investigation of kinetics of tin electrodeposition from sulphate electrolyte in the presence of sintanol DS-10. Elektrokhimiya 20:846
12. Survila A, Mockus Z, Kanapeckaitė S, Samulevičienė M (2005) Effect of sintanol DS-10 and halides on tin(II) reduction kinetics. Electrochim Acta 50:2879
13. Reid JD, David AP (1987) Effects of polyethylene glycol on the electrochemical characteristics of copper cathodes in acid copper medium. Plat Surf Finish 74:66
14. Bražinskienė D, Survila A (2005) Effect of ethylene glycol and its oligopolymers on the copper(II) electroreduction kinetics in halide-containing acid sulphate solutions. Russ J Electrochem 41:979
15. Boukamp BA (1989) Equivalent circuits (EQUIVCRT.PAS), users manual. University of Twente, The Netherlands
16. Bražinskienė D, Survila A, Samulevičienė M (2005) Cu(II) electroreduction kinetics in acidic sulphate solutions containing tetraethyleneglycol and small amounts of chlorides. Chemija (Vilnius) 16:20
17. Quintin M, Hagymas G (1964) Contribution a l'etude de la corrosion électrochimique de l'étain en milieu sulfurique. J Chim Phys 61:541
18. Kostryukova GG, Ratkov OI, Kazakov VA, Ginberg AM, Vagramyan AT (1969) On the application of relaxation methods for study of metal electrodeposition processes. I. Electrode Sn/Sn^{2+}. Elektrokhimiya 5:571
19. Galus Z (1975) Tin. In: Bard AJ (ed) Encyclopedia of electrochemistry of the elements, vol 4. Dekker, New York, pp 223–271
20. Survila A, Mockus Z, Kanapeckaitė S (2001) Voltammetric characterization of laprol 2402 C adsorption on copper and tin electrodes. Chemija (Vilnius) 12:241
21. Väärtnõu M, Lust E (2004) Impedance characteristics of iodine ions adsorption on Bi single crystal planes in ethanol. J Electroanal Chem 565:211
22. Nurk G, Kasuk H, Lust K, Jänes A, Lust E (2003) Adsorption kinetics of dodecyl sulfate anions on the bismuth (011) plane. J Electroanal Chem 553:1
23. Macdonald JR (1987) Impedance spectroscopy. Wiley, New York
24. Frumkin AN, Melik-Gaikazyan VI (1951) Determination of the kinetics of adsorption of organic substances by a.-c. measurements of the capacity and the conductivity at the boundary: electrode-solution. Dokl Akad Nauk USSR 77:855
25. Berzins T, Delahay P (1955) Electrochemical method for the kinetic study of fast adsorption processes. J Phys Chem 59:906
26. Lorenz W, Möckel F (1956) Adsorptionsisotherme und Adsorptionskinetik kapillaraktiver organischer Molekeln an der Quecksilberelektrode. Z Elektrochem 60:507
27. Sluyters-Rehbach M, Sluyters JH (1970) Sine wave methods in the study of electrode processes. In: Bard AJ (ed) Electroanal Chemistry, vol 4. Dekker, New York, pp 75–77
28. Retter U, Jehring H (1973) Untersuchungen der adsorptionskinetik an der phasengrenze quecksilber/elektrolyt durch analoge messung der doppelschichtadmittanz. J Electroanal Chem 46:375
29. Pajkossy T, Wandlowski Th, Kolb DM (1996) Impedance aspects of anion adsorption on gold single crystal electrodes. J Electroanal Chem 414:209
30. Jovič VD, Jovič BM (2003) EIS and differential capacitance measurements onto single crystal faces in different solutions: Part I: Ag(111) in 0.01 M NaCl. J Electroanal Chem 541:1
31. Brug GJ, van den Eeden ALG, Sluyters-Rehbach M, Sluyters JH (1984) The analyses of electrode impedances complicated by the presence of a constant phase element. J Electroanal Chem 176:275
32. Retter U, Widmann A, Siegler K, Kahlert H (2003) On the impedance of potassium nickel(II) hexacyanoferrate(II) composite electrodes—the generalization of the Randles model referring to inhomogenous electrode materials. J Electroanal Chem 546:87